- Supporting Information -

Cobalt doped WS_2/WO_3 Nanocomposite Electrocatalyst for the Hydrogen Evolution Reaction in Acidic and Alkaline media

*Sunil R. Kadam,[1] Ronen Bar-Ziv,[2] Maya Bar-Sadan,[1,3]**

[1]Ben-Gurion University of the Negev, Department of Chemistry, Beer-Sheva, Israel.

[2]Chemistry Department, Nuclear Research Center-Negev (NRCN), Beer Sheva 84190, Israel.

[3]Ilse Katz Institute for Nanoscale Science and Technology, Ben Gurion University, Beer Sheva Israel.

E-mail: barsadan@bgu.ac.il

1. Experimental section

Materials

All the chemicals were used as received without further purification. Ammonium metatungstate hydrate ($(NH_4)_6H_2W_{12}O_{40}\cdot xH_2O$) (STREM chemicals INC.), Dibenzyldisulfide (Alfa Aesar), Nickel (II) acetylacetonate (Acros organics), Iron (III) acetylacetonate (STREM Chemicals Inc.), Cobalt (II) acetylacetonate (Alfa Aesar), Oleylamine technical grade 70 % (Aldrich), Oleic acid 90% (Alfa Aesar). The water used for washing was de-ionized water (DW) that was passed through a Milli-Q column by Millipore, with final resistance of 18.2 MΩ cm.

Synthesis of the pristine and doped catalysts

Pristine WS_2/WO_3 composite was synthesized by simple colloidal method. All the reactions were performed using standard Schlenk line technique. At first, Sulphur precursor was prepared in a 100 mL three neck round bottom (RB) flask by adding 0.2

mmol Dibenzyl disulfide powder in 10 mL Oleylamine. Further, stirring for 20 min at 110 ºC in order to make it clear solution. The WS_2 synthesis was carried out in 100 mL three-neck RB, 0.2 mmol (49.26 mg) of Ammonium metatungstate hydrate ($(NH_4)_6H_2W_{12}O_{40} \cdot xH_2O$) were mixed with 20 mL of Oleylamine and 2 mL of Oleic acid. The mixture was degassed under vacuum at 110 °C for 30 min until a clear solution was obtained. Then the RB was backfilled with N_2 gas. Further, the reaction temperature was slowly increased to 240 ºC at 5 °C/min rate. The 0.2 mmol of Dibenzyl disulfide precursor solution (10 mL Oleylamine) at 240 ºC were added dropwise using a syringe pump with constant stirring. The total volume of the reaction mixture was 32 mL. Further, the reaction temperature is increased to 300 ºC and maintained for the next 2 hours. After completion of the reaction, the heating mantle was removed and the reaction mixture was allowed to cool naturally. The final product was collected by centrifuging and washing twice with toluene, acetone, water and ethanol each followed by vacuum drying. The dried powder sample was annealed under N_2 atmosphere at 300 ºC for 3 hours in order to remove the ligands and increase the crystallinity. Doped WS_2 samples were synthesized by the same procedure except for substitution with the doping element in the desired ratio of 5% Fe (3.53 mg), 5% Co (2.59 mg) and 5% Ni (2.56 mg).

Electrode preparation and electrochemical HER measurements

Ink for the working electrodes was prepared by dispersing 2 mg of the catalyst and 1 mg Vulcan carbon black in 550 µl of Nafion solution (prepared by mixing of 2000 µl water, 500 µl ethanol and 150 µl Nafion solution (5%)). The ink was homogenized by bath ultra-sonication for 2 min followed by probe sonication (QSONICA 125 W probe sonicator) at 40% amplitude in an interval mode of 15:5 seconds on:off cycle for additional 5 min. 3 mm glassy carbon (GC) working electrode was polished to a mirror-like finishig using alumina

slurry and then 20 µl of the homogeneous ink was drop casted onto the glassy carbon electrode to form a final loading of ~1 mg cm^{-2} and kept overnight. Standard three electrode system was used for all the electrochemical measurements. Graphite rod, saturated Ag/AgCl and glassy carbon (GC) electrode coated with the WS_2/WO_3 catalyst were used as the counter, reference and working electrodes, respectively. Polarization curves were recorded on an Ivium Technology Vertex Potentiostat/Galvanostat (V74606) and analyzed using the Ivium Soft program. The electrochemical HER measurements were performed in Argon-saturated 0.5 M H_2SO_4 and 0.5 M KOH solutions at room temperature. The electrolyte was bubbled with Ar gas for 15 minutes prior to the measurements in order to remove dissolved gases from the solution. Each electrode was pre-treated with 12 cyclic voltammetry (CV) cycles between 0 V to - 0.7 V (vs. RHE) at a scan rate of 100 mV S^{-1}. Polarization curves were recorded at a scan rate of 10 mV s^{-1} over the same potential range. During the electrochemical measurements the head space of the cell was continuously purged with Ar gas. All measurements were referred to the reversible hydrogen electrode (RHE) by using the relationship: $E_{(RHE)} = E_{(Ag/AgCl)} + E^0_{(Ag/AgCl)} + 0.059V \times pH$. Electrochemical impedance spectroscopy measurement for all the samples were carried out at identical 400 mV potential.

Cyclic voltammograms measurement in 0.5 M H_2SO_4, from 0.10 V to -0.10 V (vs. RHE) were recorded at various scan rates (20, 40, 60, 80, 100 and 120 mV S^{-1}) to estimate the double-layer capacitance.

Materials characterization

The crystallographic phase of the sample was identified by Panalytical Empyrean powder X-ray diffractometer equipped with a position-sensitive X'Celerator detector using Cu Kα radiation (λ = 1.5405 Å) operated at 40 kV and 30 mA. The surface morphologies of the synthesized sample were investigated by JEOL JSM-7400F ultrahigh resolution cold FEG-SEM. The sample for SEM was prepared by dispersing the powder in ethanol, followed

by sonication in an ultrasonic bath for 1 min and then drop-casting the dispersion on a silicon wafer. The images were recorded at 2 kV acceleration voltage at 3–4 mm sample distance. Samples were prepared by dispersing the powder in ethanol, followed by sonication in an ultrasonic bath for 2 min and then drop-casting the dispersion on a carbon coated copper grid and by subsequent drying in a vacuum. XPS data were collected using an X-ray photoelectron spectrometer ESCALAB 250 ultrahigh vacuum (1×10^{-9} bar) apparatus with an Al Kα X-ray source and a monochromator. Room temperature Raman spectroscopy were performed using a LabRAM HR Evolution Raman spectrometer with a laser wavelength of 633 nm in the back-scattering geometry. The laser power on the sample was 0.6 mW with a laser spot size of 1.3 μm.

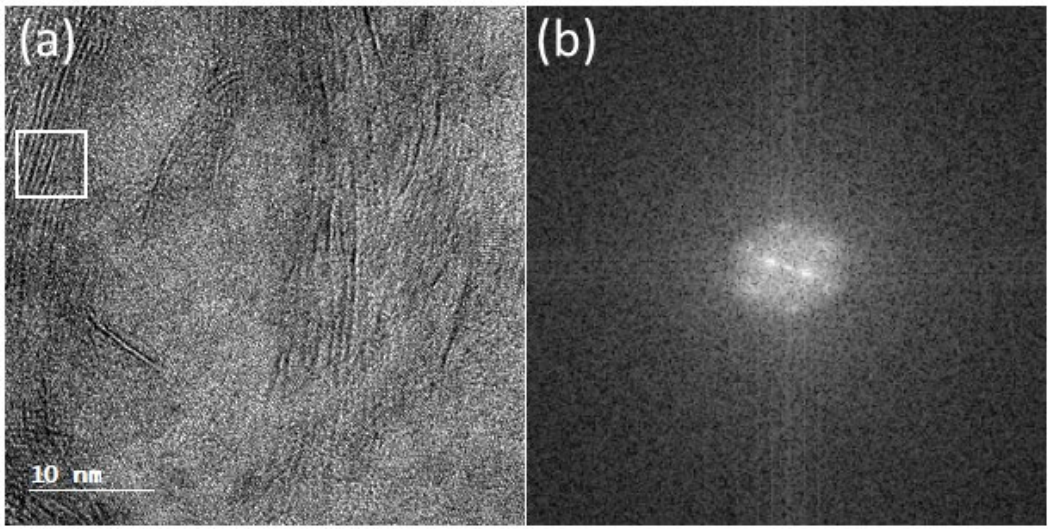

Figure S1. (a) High Resolution TEM image of pristine WS_2/WO_3 and (b) corresponding FFT pattern.

Table S1. Peak area obtained for W, S, Fe, Co and Ni from X-ray photoelectron spectroscopy

	Element	Binding Energy	Peak Area (a.u.)	Peak Area (a.u.)	W:S	1T:2H	W:Fe/Co/Ni	W^{4+}:W^{6+}
Pristine WS_2	W^{4+} 1T	31.95	1433	2208	54:46	39:61		79:21
		34.0	775					
	W^{4+} 2H	32.82	1943	3475				
		34.80	1532					
	W^{6+}	35.52	843	1508				
		37.62	665					
	S 1T	161.35	862	1527				
		162.41	441					
	S 2H	162.43	898	1358				
		163.52	460					
Fe-WS_2	W^{4+} 1T	32.06	1129	1883	69:31	24:76	94.7:5.3	83:17
		34.16	754					
	W^{4+} 2H	33.0	3232	5845				
		35.1	2613					
	W^{6+}	35.88	902	1614				
		37.98	712					
	Fe	708.4	292	531				
		721.7	239					
	S 1T	161.6	751					
		162.66	384					
	S 2H	162.68	1525					
		163.87	780					
Co-WS_2	W^{4+} 1T	32.18	1518	2719	70:30	34:66	94.9:5.1	79:21
		34.28	1201					
	W^{4+} 2H	32.96	2983	5347				
		34.06	2364					
	W^{6+}	35.84	1238	2215				
		37.94	977					
	Co	778.97	365					
		782.11	192					
	S 1T	161.62	1127.28	1704.58				
		162.68	577.3					
	S 2H	162.68	1109.51	1677.25				
		163.74	567.74					
Ni-WS_2	W^{4+} 1T	32.27	1681	3010	69:31	40:60	95.2:4.8	72:28
		34.37	1329					
	W^{4+} 2H	32.94	2492	4467				
		35.04	1975					
	W^{6+}	35.86	1630	2926				
		37.96	1286					
	Ni	856.4	366	527				

		871.5	161					
	S 1T	161.95	1904	2879				
		163.08	975					
	S 2H	163.43	313	473				
		164.49	160					

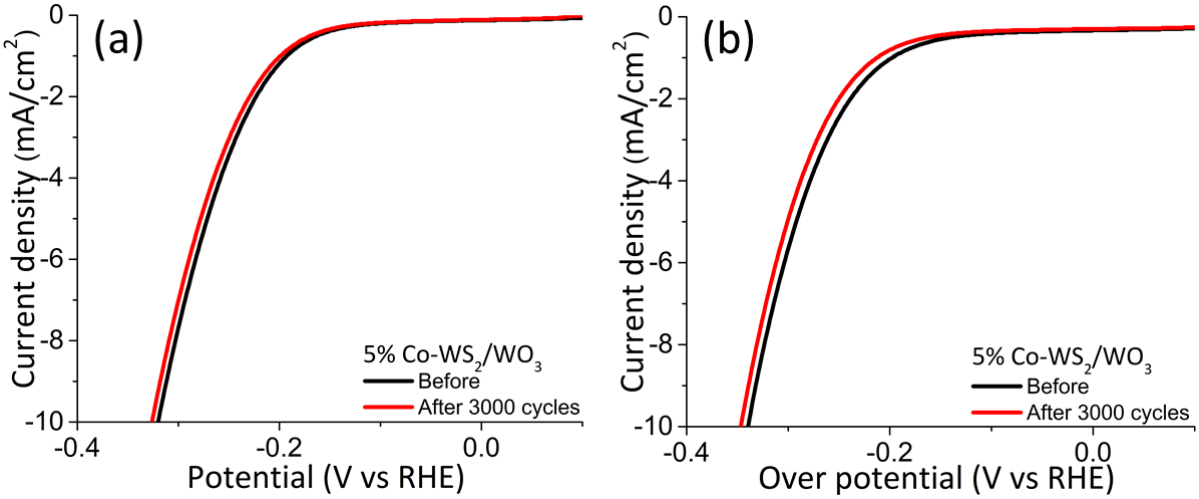

Figure S2. Stability test of 5% Co-WS_2/WO_3 sample (a) in 0.5 M H_2SO_4 and (b) in 0.5 M KOH. Polarization curves before (black) and after (red) continuous 3000 CV cycles.

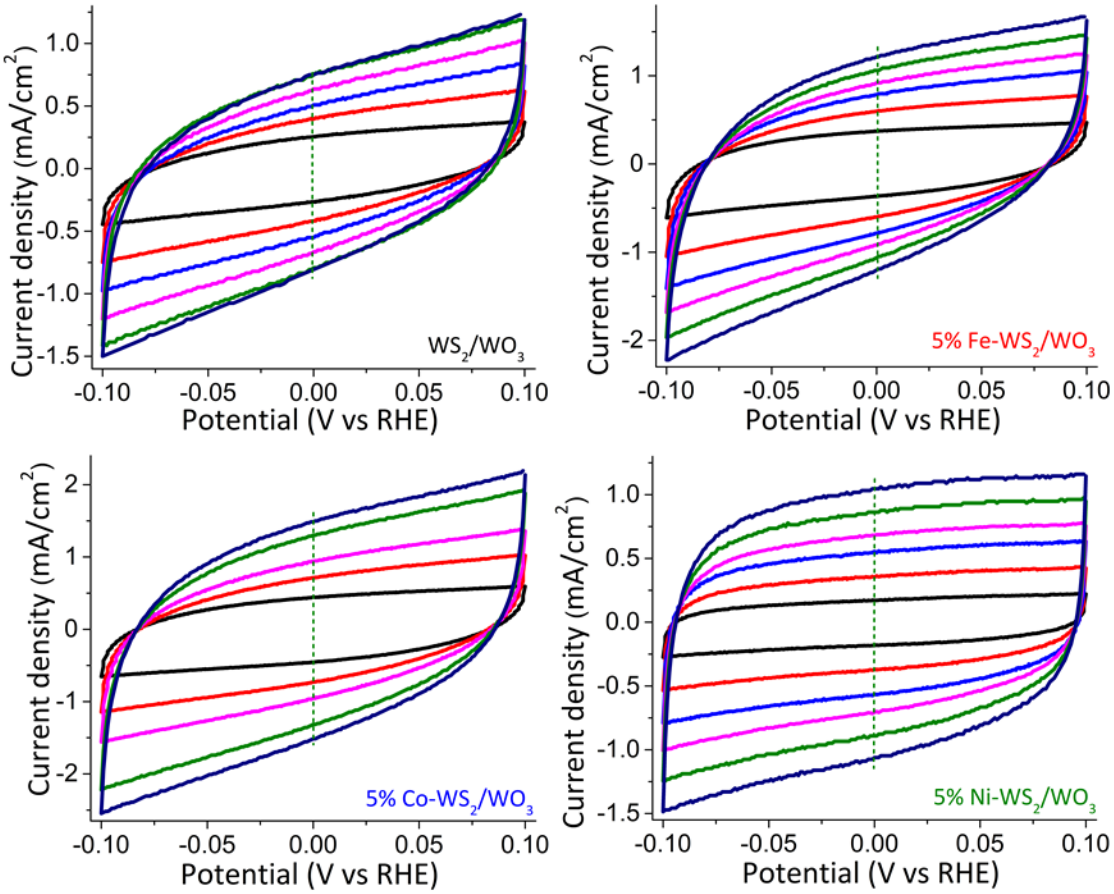

Figure S3. Cyclic voltammograms measured in non-faradaic potential region of 0.10 to -0.10 V vs. RHE for (a) Pristine WS_2/WO_3 composite (b) 5% Fe-WS_2/WO_3 (c) 5% Co-WS_2/WO_3 (c) 5% Ni-WS_2/WO_3 at various scan rates.

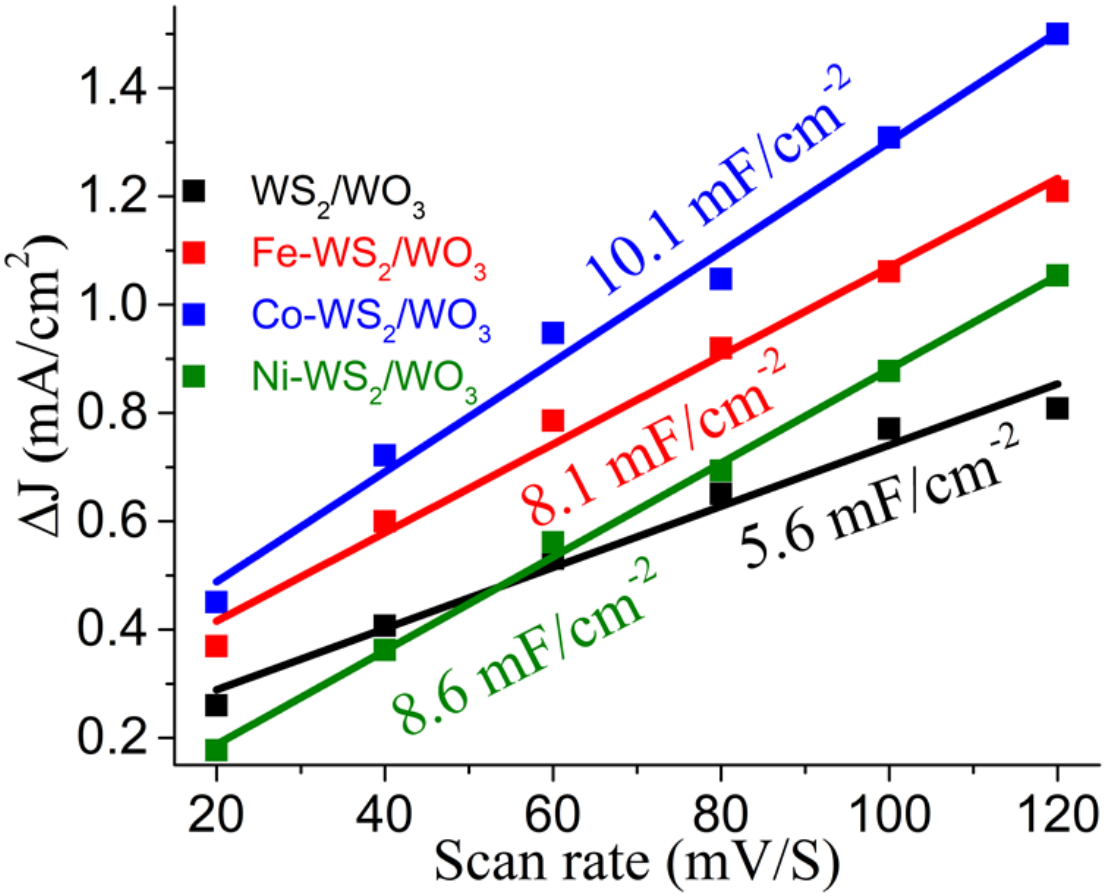

Figure S4. Linear fitting of the capacitive currents (the difference between anodic and cathodic currents, Δj) vs. scan rates to estimate the double layer capacitance (Cdl) for pristine and 5% Fe, Co and Ni doped WS_2/WO_3 composite catalysts in 0.5 M H_2SO_4.

The measured capacitance values of the samples can be converted into **electrochemical active surface area (ECSA)** using a specific capacitance of flat standard with 1cm^2 of real surface area. By taking the specific capacitance value Cs for an ideally flat standard electrode into account, Cs= 0.040 mF cm^{-2}, one can calculate ECSA = Cdl/Cs .

$$ECSA = \frac{\textbf{Specific Capacitance (mF } cm^{-2}\textbf{)}}{\textbf{0.04 mF } cm^{-2}_{ECSA}}$$

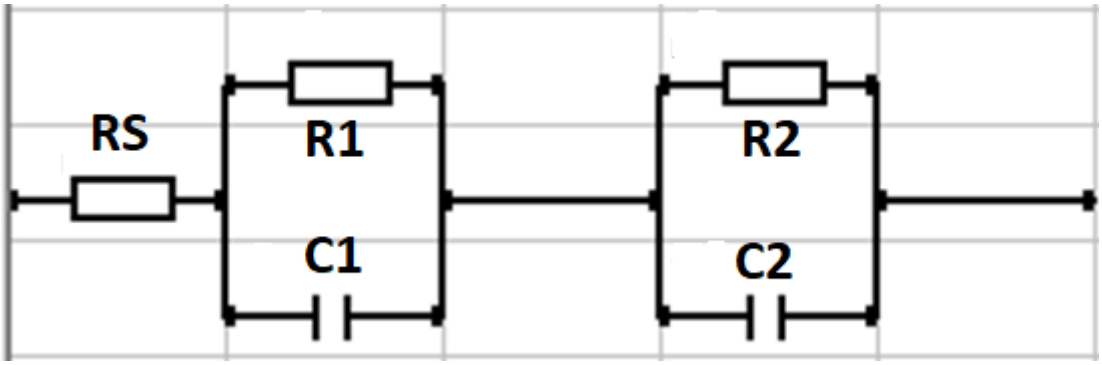

Figure S5. Equivalent circuit used to model the EIS data (Rs represent the solution's resistance, R1 represent the charge transfer resistance, R2 represent the contact between the electrode and the catalyst layer, C represent the capacitance).

Table S2. Electrochemical impedance parameters obtained by simulating the Nyquist plots to the equivalent circuit model in Figure S6.

	Rs (Ω)	**R_{ct} (Ω)**		**C (F)**	
		R_1	**R_2**	**C_1**	**C_2**
WS_2/WO_3	11.0	170.0	49.5	1.61×10^{-4}	2.78×10^{-5}
Fe- WS_2/WO_3	11.5	154.0	24.3	2.13×10^{-4}	5.30×10^{-5}
Co- WS_2/WO_3	11.9	87.5	25.9	1.49×10^{-4}	1.48×10^{-5}
Ni- WS_2/WO_3	19.3	110.8	14.0	2.85×10^{-4}	6.90×10^{-5}

Table S3. Electrochemical HER performance of present work along with previous reports.

No.	Sample	Electrolyte	Over Potential (V), η at 10 mA cm^{-2}	Tafel slope ($mV^{.}dec^{-1}$)	Reference
1	Bulk WS_2	0.5 M H_2SO_4	-0.830	-	[1]
2	exfoliated WS_2	0.5 M H_2SO_4	-0.380	-	[1]
3	WS2 sheets	0.5 M H_2SO_4	-0.382	197	[2]
4	Te-doped WS_2	0.5 M H_2SO_4	-0.213	94	[2]
5	Nb-doped WS_2	0.5 M H_2SO_4	-0.750	167	[3]
6	Ta-doped WS_2	0.5 M H_2SO_4	-0.760	175	[3]
7	1T WS_2 Monolayer	0.5 M H_2SO_4	-0.325	100	[4]
8	2H WS_2 Monolayer	0.5 M H_2SO_4	-0.684	--	
9	$2H_{1T}$ WS_2 Monolayer	0.5 M H_2SO_4	-0.515	103	
10	V single atom at 1T WS_2 monolayer	0.5 M H_2SO_4	-0.185	61	
11	WS_2 on Hollow N-Carbon nanofiber	0.5 M H_2SO_4	-0.370	110	[5]
12	2H WS_2	0.5 M H_2SO_4	-0.290	99.4	[6]
13	1T Dominant phase WS_2	0.5 M H_2SO_4	-0.200	50.4	[6]
14	Co-WS_2	0.5 M H_2SO_4	-0.255	79	[7]
15	V-WS_2 on Carbon cloth	0.5 M H_2SO_4	-0.148	72	[8]
16	WS_2/WO_3	0.5 M H_2SO_4	-0.395	50	[9]
17	WS_2/W_2C@NSPC	0.5 M H_2SO_4	-0.125	68	[10]
18	WS_2/W_2C@NSPC	1 M KOH	-0.205	72	[10]
19	1T WS_2/CC	1 M KOH	-0.319	190	[11]
20	400WS/CC	1 M KOH	-0.235	174	[11]
21	Co_9S_8/WS_2	1 M KOH	-0.138	80.2	[12]
22	***5% Co-WS_2***	***0.5 M H_2SO_4***	***-0.321***	***108***	***Present Work***
		0.5 M KOH	***-0.337***	***136***	

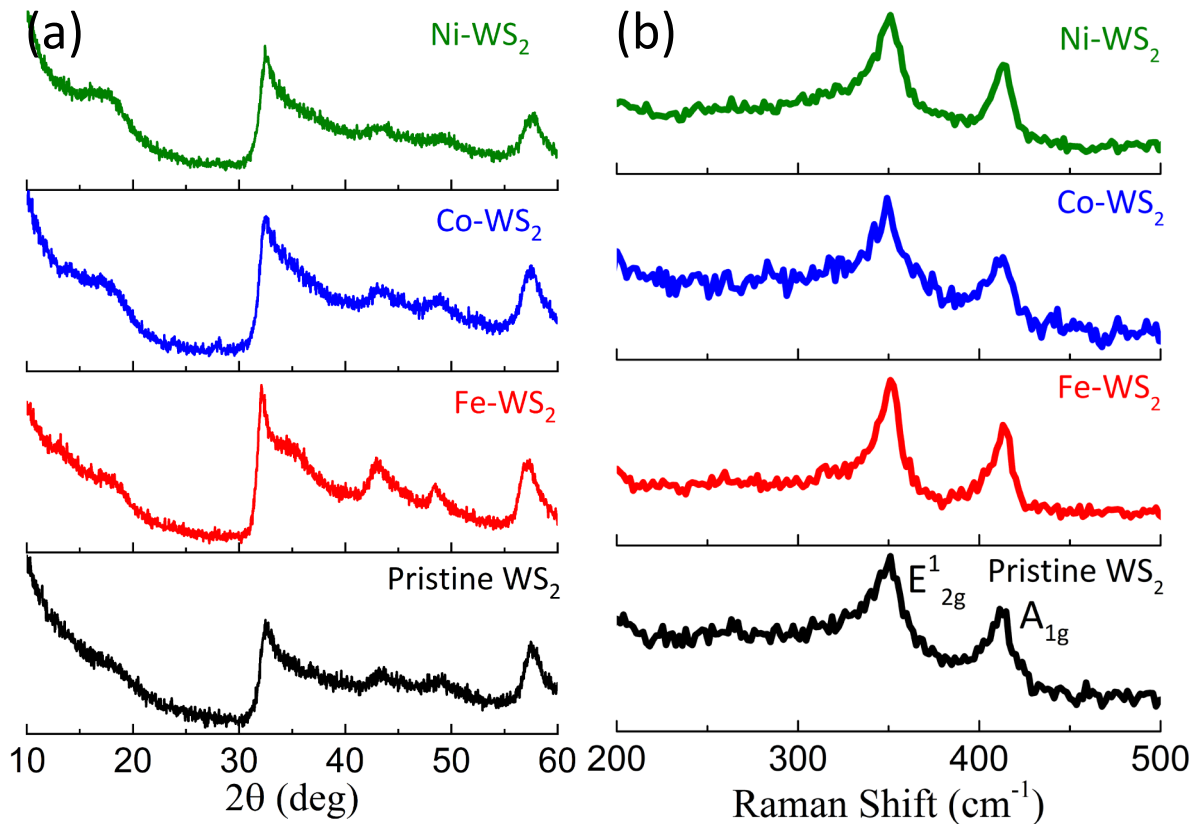

Figure S6. (a) XRD patterns of the as prepared (before annealing) pristine WS_2/WO_3 composite, and 5% of Fe, Co and Ni-doped WS_2/WO_3 composite. (b) Corresponding Raman spectra of the samples set. Raman measurements were carried out using an excitation laser wavelength of 633 nm.

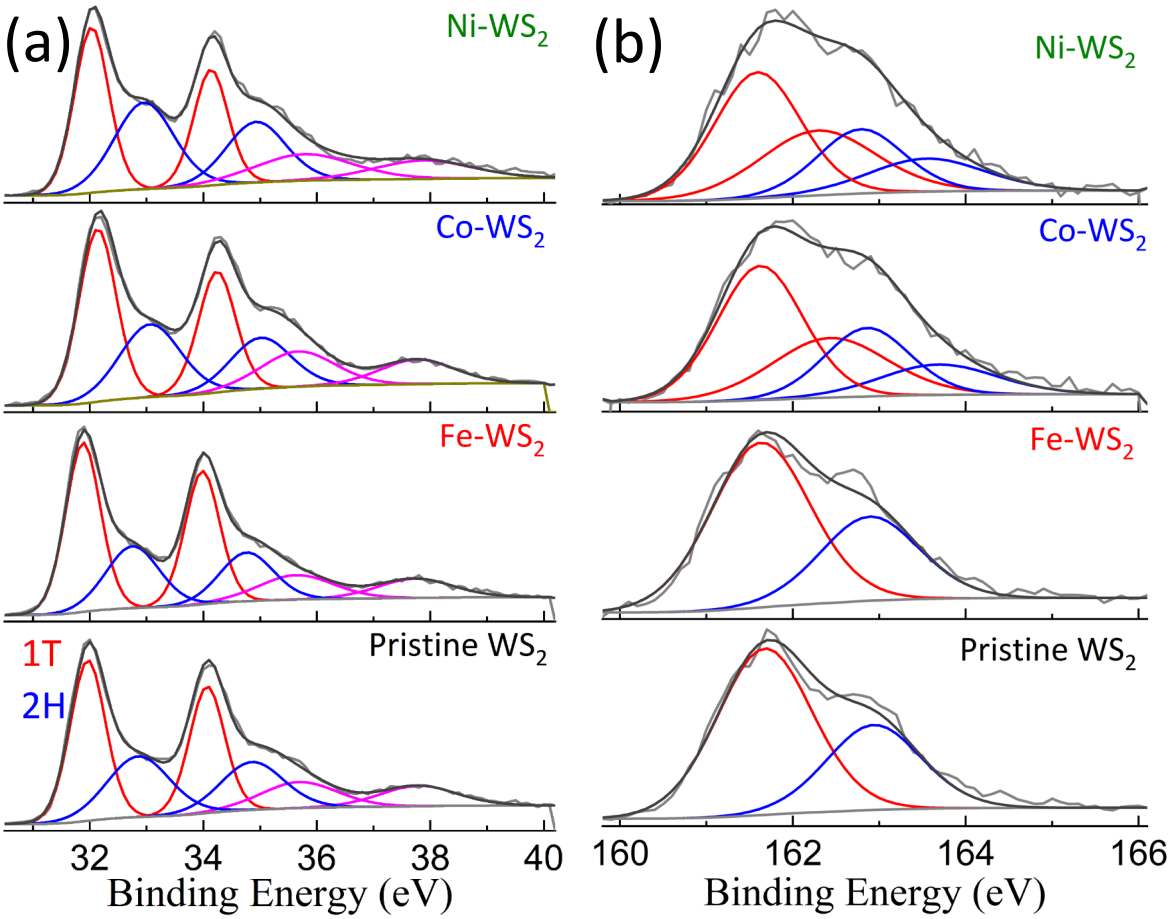

Figure S7. X-ray photoelectron spectra of (a) W 4f and (b) S 2p for as prepared (before annealing) pristine WS_2/WO_3 composite along with 5 % Fe, Ni and Co-doped WS_2/WO_3 composite

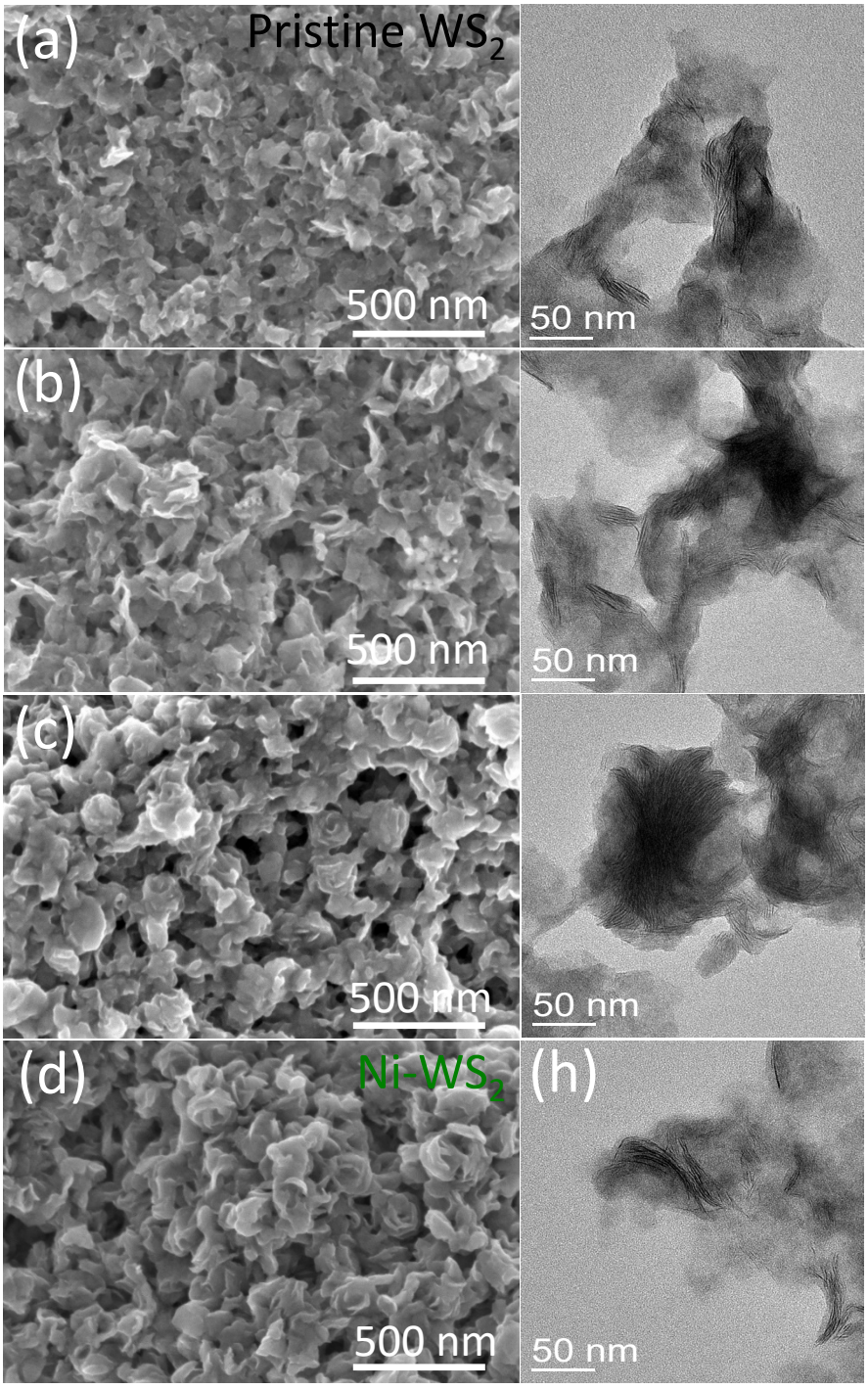

Figure S8. (a)SEM and TEM images of the as prepared (before annealing) pristine WS_2/WO_3 composite and its doped variants with 5% of Fe, Co, and Ni.

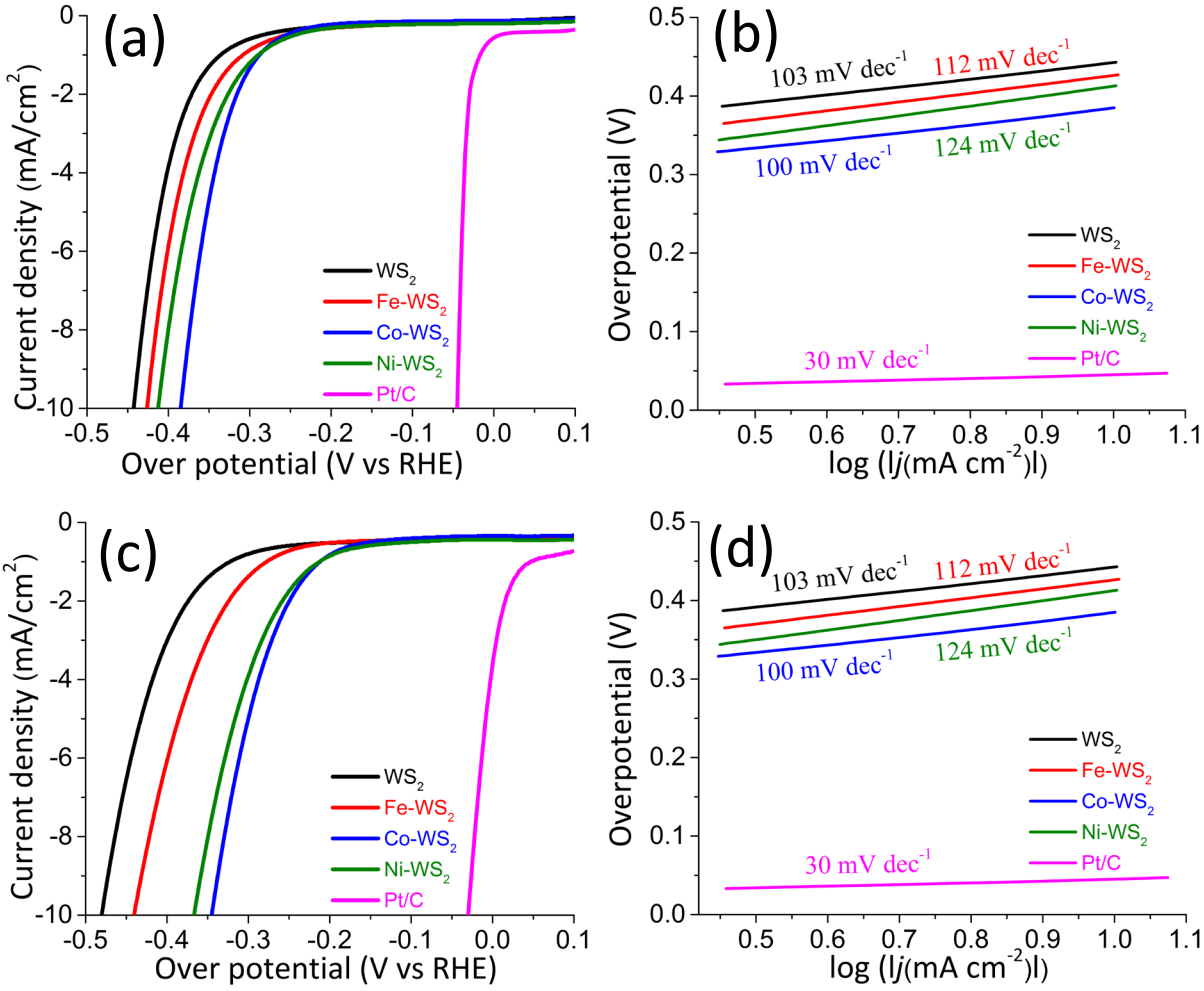

Figure S9. (a) HER polarization curves of as prepared (before annealing) pristine WS_2/WO_3 composite and 5% Fe, Co, Ni-doped composite catalysts in 0.5 M H_2SO_4 (b) corresponding Tafel plots obtained from the polarization curves (c) HER polarization curves of pristine and doped composite catalysts in 0.5 M KOH (d) corresponding Tafel plots obtained from the polarization curves.

Table S4: The electrochemical HER results for various composite samples in acidic and alkaline media.

Catalyst	Over Potential at 10 mA/cm^2 (mV)	Over Potential at 10 mA/cm^2 (mV)	Tafel slope (mV/dec)	Tafel slope (mV/dec)
	Acid	Base	Acid	Base
Pristine WS_2	443	482	103	153
5% Fe-WS_2	427	441	112	159
5% Co-WS_2	385	345	100	125
5 % Ni-WS_2	413	368	124	150

References

1. A. Ambrosi, Z. e. Sofer and M. Pumera, *Chem. Commun.*, 2015, **51**, 8450-8453.
2. Y. Pan, F. Zheng, X. Wang, H. Qin, E. Liu, J. Sha, N. Zhao, P. Zhang and L. Ma, *J. Catal.*, 2020, **382**, 204-211.
3. X. J. Chua, J. Luxa, A. Y. S. Eng, S. M. Tan, Z. k. Sofer and M. Pumera, *ACS Catal.*, 2016, **6**, 5724-5734.
4. A. Han, X. Zhou, X. Wang, S. Liu, Q. Xiong, Q. Zhang, L. Gu, Z. Zhuang, W. Zhang, F. Li, D. Wang, L.-J. Li and Y. Li, *Nat Commun*, 2021, **12**, 709.
5. S. Yu, J. Kim, K. R. Yoon, J.-W. Jung, J. Oh and I.-D. Kim, *ACS Appl. Mater. Interfaces*, 2015, **7**, 28116-28121.
6. Z. Liu, N. Li, C. Su, H. Zhao, L. Xu, Z. Yin, J. Li and Y. Du, *Nano Energy*, 2018, **50**, 176-181.
7. L. Zhou, S. Yan, H. Song, H. Wu and Y. Shi, *Sci Rep*, 2019, **9**, 1357.
8. A. Jiang, B. Zhang, Z. Li, G. Jin and J. Hao, *Chem. Asian J.*, 2018, **13**, 1438-1446.
9. X. Shang, Y. Rao, S.-S. Lu, B. Dong, L.-M. Zhang, X.-H. Liu, X. Li, Y.-R. Liu, Y.-M. Chai and C.-G. Liu, *Mater. Chem. Phys.* , 2017, **197**, 123-128.
10. Y. Li, X. Wu, H. Zhang and J. Zhang, *ACS Appl. Energy Mater.*, 2018, **1**, 3377-3384.
11. Q. Zhu, W. Chen, H. Cheng, Z. Lu and H. Pan, *ChemCatChem*, 2019, **11**, 2667-2675.
12. S. Peng, L. Li, J. Zhang, T. L. Tan, T. Zhang, D. Ji, X. Han, F. Cheng and S. Ramakrishna, *J. Mater. Chem. A*, 2017, **5**, 23361-23368.